Available online at www.sciencedirect.com
ScienceDirect
Journal of Hazardous Materials 152 (2008) 263–275
Journal of Hazardous Materials
www.elsevier.com/locate/jhazmat

Treatment of wastewater containing toxic chromium using new activated carbon developed from date palm seed

Ahmed El Nemr*, Azza Khaled, Ola Abdelwahab, Amany El-Sikaily

Department of Pollution, Environmental Division, National Institute of Oceanography and Fisheries, El-Anfoushy, Kayet Bey, Alexandria, Egypt

Received 28 February 2007; received in revised form 26 May 2007; accepted 27 June 2007
Available online 30 June 2007

Abstract

The use of a new activated carbon developed from date palm seed wastes, generated in the jam industry, for removing toxic chromium from aqueous solution has been investigated. The activated carbon has been achieved from date palm seed by dehydrating methods using concentrated sulfuric acid. The batch experiments were conducted to determine the adsorption capacity of the biomass. The effect of initial metal concentration (25–125 mg l^{-1}), pH, contact time, and concentration of date palm seed carbon have been studied at room temperature. A strong dependence of the adsorption capacity on pH was observed, the capacity increase as pH value decrease and the optimum pH value is pH 1.0. Kinetics and adsorption equilibrium were studied at different sorbent doses. The adsorption process was fast and the equilibrium was reached within 180 min. The maximum removal was 100% for 75 mg l^{-1} of Cr^{6+} concentration on 4 g l^{-1} carbon concentration and the maximum adsorption capacity was 120.48 mg g^{-1}. The kinetic data were analyzed using various kinetic models – pseudo-first order equation, pseudo-second order equation, Elovich equation and intraparticle diffusion equation – and the equilibrium data were tested using several isotherm models, Langmuir, Freundlich, Koble–Corrigan, Redlich–Peterson, Tempkin, Dubinin–Radushkevich and Generalized isotherm equations. The Elovich equation and pseudo-second order equation provide the greatest accuracy for the kinetic data and Koble–Corrigan and Langmuir models the closest fit for the equilibrium data. Activation energy of sorption has also been evaluated as 0.115 and 0.229 kJ mol^{-1}.

Keywords: Date palm seed; Activated carbon; Toxic chromium; Kinetics; Isotherm; Adsorption; Wastewater

1. Introduction

The removal of toxic heavy metal contaminants from wastewater is currently one of the most important environmental issues being researched. Although it has been studied for many years, effective treatment options are still needed. Chemical precipitation, reduction, ion exchange, filtration, electrochemical treatment, membrane technology, reverse osmosis, evaporation removal and solvent extraction are the methods most commonly used for removing toxic metals ions from wastewater [1]. However, most of these technology processes have considerable disadvantages including incomplete metal removal, requirements for expensive equipment, monitoring system and reagent or energy requirements or producing of toxic sludge or other disposal waste products [2–4].

Adsorption is found to be an important basis for the removal of toxic pollutants from wastewater. It is by far the most widely used technique for the removal of toxic metal ions from wastewater. Many reports have been appeared on the production of low cost adsorbents using cheaper and readily available materials [5–12]. Activated carbon has versatility and wide range of applications and it has been proven to be an effective adsorbent for the removal of a wide variety of organic and inorganic pollutants from different media [5,13]. Activated carbon is classified based on its size shape into four types: powder, granular, fibrous, and clothe and each type of them has its specific application as well as inherent advantages and disadvantages in wastewater treatment. Therefore, production of low-cost activated carbon becomes a great goal of many researchers since the commercial activated carbon is still very expensive [5].

Chromium has a priority metal pollutant and exists primarily in aqueous solution mainly in trivalent and hexavalent oxidation states. The former is relatively non-toxic and an essential trace nutrient in the human diet as well as it is believed by many

* Corresponding author. Tel.: +20 3 5740944; fax: +20 3 5740944.
E-mail address: ahmedmoustafaelnemr@yahoo.com (A. El Nemr).

0304-3894/$ – see front matter © 2007 Elsevier B.V. All rights reserved.
doi:10.1016/j.jhazmat.2007.06.091

to play a pharmaceutical role in the human body, while the later is highly toxic, being a mutagen and a potential carcinogen [14–16]. Several species can be obtained from hexavalent chromium by change the concentration and pH of chromium solution. At pH > 7, the CrO_4^{2-} form will preferably exists in the solution, while in the pH between 1 and 6, $HCrO_4^{2-}$ is predominant. Therefore, within the normal pH range in natural waters, the CrO_4^{2-}, $HCrO_4^{2-}$ and $Cr_2O_7^{2-}$ ions are the expected forms of hexavalent chromium in the solution, which are quite soluble and mobile in water streams [14,16]. Accidental chromium ingestion causes stomach upsets, ulcers, kidney and liver damages and even death [15,17]. Trivalent chromium (Cr^{3+}) occurs naturally in rocks, soil, plants, animals, and volcanic emissions and it is used industrially as a brick lining for high-temperature industrial furnaces and to make metals, metal alloys, and chemical compounds. Hexavalent chromium (Cr^{6+}) is produced industrially when Cr^{3+} is heated in the presence of mineral bases and atmospheric oxygen [18,19]. The maximum permissible levels sited by US regulations for chromium discharges are 0.05 mg l^{-1} of Cr^{6+} and the USEPA drinking water regulations limit the total chromium in drinking water to less than or equal to 0.1 mg l^{-1} [20,21]. Therefore, removal of toxic chromium from effluents in an economic method is a major problem for many industries.

In our laboratory, we are enthusiastic to develop different kinds of activated carbons from low-cost materials such as agriculture wastes and marine plants as well as investigate its applicability to remove hazard materials from water and wastewater. This study was to develop new activated carbon from date palm seed and to evaluate its capacity to remove toxic chromium from different aqueous solutions. Batch adsorption process has been used to evaluate the maximum adsorption capacity of activated carbon produced from date palm seed by acid dehydration. The main parameters considered are pH, contact time, initial metal ions concentration and sorbent concentration. The interference of the saline water and wastewater on the adsorption of Cr^{6+} was also investigated.

2. Materials and methods

2.1. Biomass

Date palm seed was collected from the jam industries of the north part of Egypt and washed with tap water, distilled water and oven dried at 200 °C for 24 h. The dried seed was milled, sieved and the particles ≤0.5 mm was selected for carbonization.

2.2. Carbonization of date palm seed (DSC)

Dried date palm seed (2.0 kg) was added in small portion to H_2SO_4 (98%, 2.0 l) during 5 h followed by boiling for 20 h in a fume hood. Cool in ice bath and the reaction mixture was poured onto cold water (5 l) and filtered. The obtained carbon was dried in an open oven at 120 °C for 24 h followed by immersed in 5% $NaHCO_3$ (4.0 l) to remove any remaining acid and then filter. The produced carbon was then washed with distilled water until pH of the activated carbon reached 6, dried at 150 °C for 24 h and sieved to the particle size ≤0.100 mm and kept in a glass bottle until used.

2.3. Preparation of artificial wastewater

A stock solution of 2.0 g l^{-1} was prepared by dissolving the 5.657 g of potassium dichromate ($K_2Cr_2O_7$) in 500 ml and completed to 1000 ml with distilled water. Concentrations ranged between 5 and 150 mg l^{-1} were prepared from the stock solution to have the standard curve. Double-distilled water was used for preparing all of the solutions and reagents and the pH values are adjusted with 0.1 M HCl or 0.1 M NaOH. All the adsorption experiments were carried out at room temperature (25 ± 2 °C) and analytical-grade reagents were used throughout this study.

2.4. Simulation studies

Synthetic seawater was prepared by dissolving 35 g of NaCl in 1000 ml distilled water and the resulting solution was used instead of distilled water. Different concentrations of Cr^{6+} were prepared from the synthetic seawater [7].

Natural seawater was collected from Eastern Harbor, Alexandria, Egypt and filtered using Whatman filter paper. The clear natural seawater was used instead of distilled water to prepare different concentrations of Cr^{6+} [7].

Wastewater was collected from El-Emoum drain (contains several industrial effluents and agriculture drain from Alexandria Governorate) near lake Maruit, Alexandria, Egypt. The collected wastewater was filtered through Whatman filter paper to remove suspended particulates and used as above for preparing of different concentrations of Cr^{6+} [7].

2.5. Batch biosorption studies

2.5.1. Effect of pH on Cr^{6+} adsorption

The effect of initial pH on the chromium ions adsorption onto DSC was carried out at 75 mg l^{-1} initial Cr^{6+} concentration with 0.5 g/100 ml DSC mass at 25 ± 2 °C for 3 h equilibrium time. The initial pH values were adjusted to 1.0, 2.2, 3.1, 4.4, 5.4, 6.2 and 7.2 with 0.1 M HCl or 0.1 M NaOH. The suspensions were shaken using agitation speed (200 rpm) for 3 h and the amount of Cr^{6+} ions adsorbed were determined.

2.5.2. Effect of activated carbon dose

The effect of DSC dose on the uptake of Cr^{6+} was investigated using DSC concentrations of 1, 2, 3, 4 and 5 g l^{-1}. The experiments were achieved by shaking known concentration of Cr^{6+} with the above DSC dose for 3 h and the amount of Cr^{6+} adsorbed determined.

2.5.3. Kinetics studies

Kinetics studies were performed in 300 ml conical flasks at solution pH 1.0 by mixing of DSC (0.1, 0.2, 0.3, 0.4 and 0.5 g) with 100 ml of Cr^{6+} solution (25–125 mg l^{-1}) and shaken at room temperature (25 ± 2 °C) for 3 h. Samples of 1.0 ml were

collected from the duplicate flasks at required time intervals 5–180 min and centrifuged for 5 min. The clear solutions were analyzed for residual Cr^{6+} concentration in the solution.

2.5.4. Adsorption isotherm

Batch sorption experiments were carried out at room temperature by agitating DSC (0.1, 0.2, 0.3, 0.4 and 0.5 g) with 100 ml of Cr^{6+} (25–125 mg l^{-1}) for 3 h at pH 1.0 and then the reaction mixture was analyzed for the residual Cr^{6+} concentration.

The concentration of Cr^{6+} in solution was measured according to standard method introduced by Gilcreas et al. [22] using UV–vis spectrophotometer (Milton Roy, Spectronic 21D) using silica cells of path length 1.0 cm at wavelength λ 540 nm. All the experiments are duplicated and only the mean values are reported. The maximum deviation observed was less than 5%. Adsorption of Cr^{+6} was studied using different weights of DSC in 100 ml solution of 25, 50, 75, 100 and 125 mg l^{-1} of initial Cr^{6+} concentration and initial pH 1.0.

The amount of Cr^{+6} adsorbed onto carbon, q_e (mg g^{-1}), was calculated by the following mass balance relationship:

$$q_e = \frac{(C_0 - C_e) \times V}{W} \quad (1)$$

where C_0 and C_e are the initial and equilibrium liquid-phase concentrations of Cr^{+6}, respectively (mg l^{-1}), V the volume of the solution (l), and W is the weight of the DSC used (g).

3. Results and discussion

3.1. Influence of solution initial pH

The wastewater from industries usually has a wide range of pH values. The effect of pH was determined by studying adsorption of Cr^{6+} at an initial Cr^{6+} concentration of 75 mg l^{-1} with adsorbent doses of 0.5 g/100 ml for DSC over a pH range of 1–7.2. Fig. 1 shows the effect of pH on the adsorption of Cr^{6+} by DSC. Maximum adsorption was noticed at pH 2 (100%). When initial pH of the solution was increased from 1.0 to 5.35, the percentage removal decreased from 100 to 25.3%. With increase in pH from 5.35 to 7.2, the percent removal was slightly increased from 25.35 to 27.2%, which may be attributed to some coagulation or precipitation of chromium. Maximum adsorption of Cr^{6+} occurred at low pH can be explained by the species of the chromium and the functional group present in the adsorbent surface. At pH above 8, the predominant species is CrO_4^{2-} and with the increase of the acidity the equilibrium shifts to dichromate formation and the predominant species of chromium at acidic pH are $Cr_2O_7^{2-}$, $HCrO_4^-$, $Cr_3O_{10}^{2-}$ and $Cr_4O_{13}^{2-}$ [23–25]. On the other hand, under acidic conditions, the surface of the adsorbent becomes highly protonated that favors the uptake of Cr^{6+} in the anionic form. Increase in pH value (move toward basic solution) causes decrease in protonation of the surface, which led to decrease in net positive surface potential of sorbent. This decrease the electrostatic forces between sorbent and sorbate that leads to reduced sorption capacity [26]. Moreover, as pH value increases there is competition between OH^- and chromate ions.

3.2. Influence of contact time

The relation between adsorption of Cr^{6+} and contact time were investigated to identify the rate of chromium removal. Fig. 2 shows the percentage removal of Cr^{6+} at different initial chromium concentrations ranging from 25 to 125 mg l^{-1} and pH 1.0. It was found that more than 40% removal of Cr^{6+} concentration occurred in the first 45 min, and thereafter the rate of adsorption was found to be slow. The removal of Cr^{6+} by DSC ranged from 70 to 100% with various initial chromium concentrations. The equilibrium time was 180 min and after that, percentage removal was more or less constant. Therefore, it can be concluded that the rate of Cr^{6+} binding with adsorbent was greater in the initial stages, then gradually decreased and remained almost constant after an optimum period. The slow rate of Cr^{6+} adsorption after the first 45 min is probably occurred due to the slow pore diffusion of the solute ion into the bulk of the adsorbent.

3.3. Influence of initial chromium concentration

The adsorption experiments at initial chromium concentrations from 25 to 125 mg l^{-1} were also performed with DSC

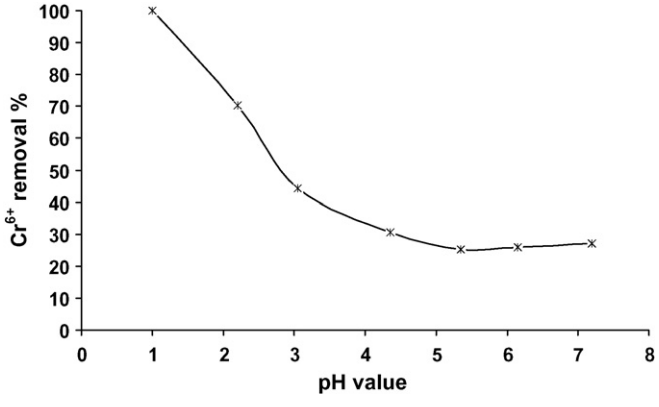

Fig. 1. Effect of system pH on adsorption of Cr^{6+} (75 mg l^{-1}) onto DSC (0.5 g/100 ml) at 27 ± 2 °C.

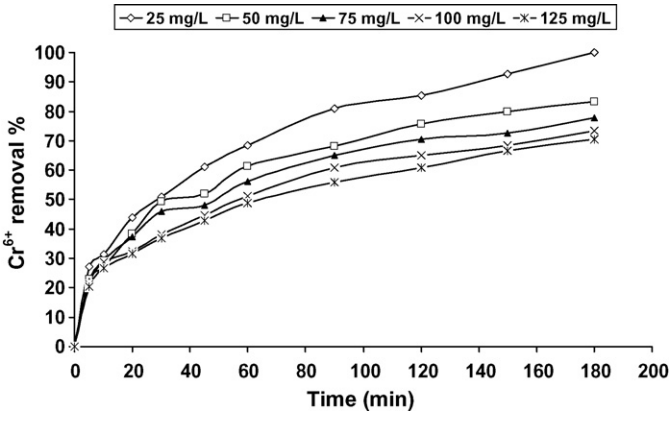

Fig. 2. Effect of contact time on the removal of different initial concentrations of Cr^{6+} using DSC (0.2 g/100 ml) at pH 1.0.

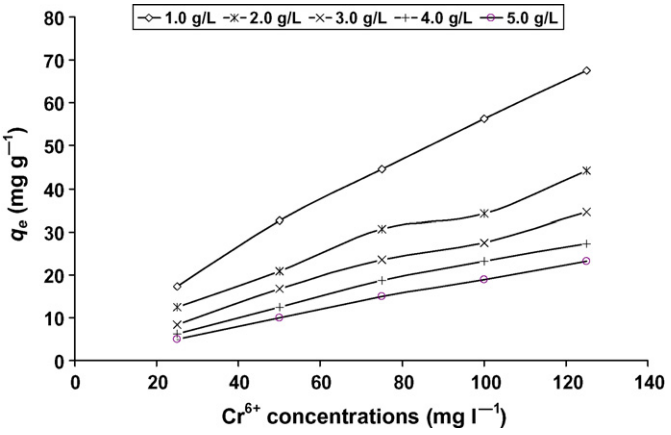

Fig. 3. Relation between amounts of chromium (Cr^{6+}) adsorbed at equilibrium (q_e) and its initial concentration using different doses of DSC.

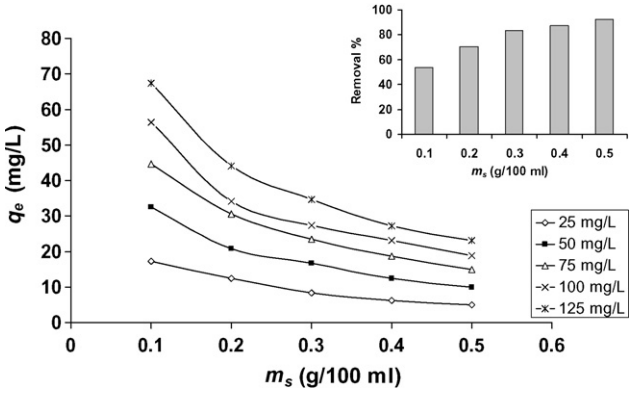

Fig. 4. Inside figure: effect of DSC concentration on Cr^{6+} removal (C_0: 125 mg l^{-1}, pH 1.0, agitation speed: 200 rpm, temperature: 27 ± 2 °C). Main figure: effect of mass (m_s) of DSC concentration on q_e of Cr^{6+} (C_0: 25–125 mg l^{-1}, pH 1.0, agitation speed: 200 rpm, temperature: 27 ± 2 °C).

doses (0.1, 0.2, 0.3, 0.4 and 0.5 g/100 ml) and the results are represented in Figs. 1 and 3. The results indicate that percentage Cr^{6+} removal decreases as the initial concentration of Cr^{6+} was increased. This can be explained by the fact that all the adsorbents had a limited number of active sites, which would have become saturated above a certain concentration. Increase of the initial metal concentration results in a decrease in the initial rate of external diffusion and increase in the intraparticle diffusion rate.

In the process of Cr^{6+} adsorption, first metal ions have to encounter the boundary layer effect and then diffuse from boundary layer film onto DSC surface and finally, it has to diffuse into the porous structure of the DSC. This phenomenon will take relatively longer contact time. Fig. 3 shows that the amount of Cr^{6+} adsorbed on DSC at a lower initial concentration of chromium was smaller than the corresponding amount when higher initial concentrations were used. On the other hand, the percentage removal of chromium was higher at lower initial chromium concentrations and smaller at higher initial concentrations, which clearly indicate that the adsorption of Cr^{6+} from its aqueous solution was dependent on its initial concentration.

3.4. Influence of carbon concentration on metal adsorption

To determine the influence of DSC dosage on the amount of adsorption, the DSC mass was varied from 0.1 to 0.5 g/100 ml, while initial chromium concentration was held constant at 125 mg l^{-1} at room temperature (Fig. 4: inside figure). The percentage of metal removal increased with increasing DSC dosage at the same initial metal concentration. On the other hand, the quantity of metal adsorbed was studied and represented in Fig. 4 (main figure), which shows that the amount of chromium adsorbed at equilibrium, q_e, decreases with increase of DSC dose, while it increases with increase of initial metal concentration for all studied dose of DSC. The increase in metal removal with the adsorbent dose can be attributed to increased surface area and the sorption sites. However, the decrease in adsorption capacity can be explained with the reduction in the effective surface area.

3.5. Adsorption isotherm investigation

The equilibrium study on adsorption has provided sufficient information on the capacity of the adsorbent. Also, an adsorption isotherm is characterized by certain constant values that express the surface properties and affinity of the adsorbent and can also be used to compare the adsorptive capacities of the adsorbent for different pollutants. Equilibrium data should accurately fit into different isotherm models to find a suitable model that can be used for the design process [27]. To establish the adsorption capacity of DSC various isotherm equations have been tested in the present study. These equations are Langmuir, Freundlich, Koble–Corrigan, Redlich–Peterson, Tempkin, Dubinin–Radushkevich and Generalized isotherm equations. The applicability of isotherm equations is compared by judging the correlation coefficients.

3.5.1. Langmuir isotherm

The Langmuir isotherm [28,29] has been used extensively by many authors for the adsorption of heavy metals, dyes, organic pollutant and gases onto activated carbon, clay, agriculture wastes, etc. It is valid for monolayer adsorption on specific homogenous sites containing a finite number of identical sites and it assumes uniform energies of adsorption on the surface and no transmigration of sorbate in the plane of the surface [30,31]. The Langmuir isotherm model estimates the maximum adsorption capacity produced from complete monolayer coverage on the adsorbent surface. The non-linear equation of Langmuir isotherm model can be expressed in the following non-linear form:

$$q_e = \frac{Q_m K_a C_e}{1 + K_a C_e} \quad (2)$$

where C_e and q_e are as defined above in Eq. (1); K_a the adsorption equilibrium constant (l mg^{-1}) that is related to the apparent energy of adsorption; Q_m is the maximum monolayer capacity of the adsorbent (mg g^{-1}). Eq. (2) can be linearized into four different forms as shown in Table 1 (Eqs. (3)–(6)), which give different possibilities to parameter estimation [32,33].

Table 1
The four linear forms of Langmuir isotherm model

Form	Linear equation	Plot	Slope	Intercept
Langmuir-1	$\frac{C_e}{q_e} = \frac{1}{K_a Q_m} + \frac{1}{Q_m} \times C_e$ (3)	C_e/q_e vs. C_e	$1/Q_m$	$1/(K_a Q_m)$
Langmuir-2	$\frac{1}{q_e} = \left(\frac{1}{K_a Q_m}\right)\frac{1}{C_e} + \frac{1}{Q_m}$ (4)	$1/q_e$ vs. $1/C_e$	$1/(K_a Q_m)$	$1/Q_m$
Langmuir-3	$q_e = Q_m - \left(\frac{1}{K_a}\right)\frac{q_e}{C_e}$ (5)	q_e vs. q_e/C_e	$1/K_a$	Q_m
Langmuir-4	$\frac{q_e}{C_e} = K_a Q_m - K_a q_e$ (6)	q_e/C_e vs. q_e	K_a	$K_a Q_m$

Table 2
Isotherm parameters obtained from the four linear forms of Langmuir model for the adsorption of Cr^{6+} onto activated carbon developed date palm seed

Isotherm model	Isotherm parameters	Date seed activated carbon concentrations	
		1.0 g l^{-1}	2.0 g l^{-1}
Langmuir-1	Q_m (mg g^{-1})	120.48	63.69
	$K_a \times 10^3$ (l mg^{-1})	20.70	62.03
	R^2	0.983	0.994
Langmuir-2	Q_m (mg g^{-1})	112.36	69.93
	$K_a \times 10^3$ (l mg^{-1})	23.21	53.88
	R^2	0.999	0.987
Langmuir-3	Q_m (mg g^{-1})	115.52	64.64
	$K_a \times 10^3$ (l mg^{-1})	22.27	60.35
	R^2	0.968	0.942
Langmuir-4	Q_m (mg g^{-1})	117.66	66.71
	$K_a \times 10^3$ (l mg^{-1})	21.60	56.80
	R^2	0.968	0.942

The results obtained from Langmuir model for the removal of Cr^{6+} onto DSC are represented in Table 2. The correlation coefficients for the all linear forms of Langmuir model are $R^2 > 0.94$ with forms 1 and 2 being the best fitted for the equilibrium data site $R^2 \geq 0.983$. Fig. 5 shows the plot of Langmuir-2 isotherm model and Fig. 6 represents comparison between the experimental data measured and modeled Langmuir equilibrium isotherms of Cr^{6+} adsorption on various dose of DSC. The maximum monolayer capacity Q_m obtained from Langmuir model was 120.48 mg l^{-1}. This value is comparable to the adsorption capacities of some other adsorbent materials [5].

3.5.2. Freundlich isotherm

The Freundlich isotherm theory is the first known relationship explains the adsorption process [34]. It describes the ratio of the amount of solute adsorbed onto a given mass of sorbent to the concentration of the solute in the solution is not constant at different concentrations. Freundlich isotherm equation is applicable to the adsorption on heterogeneous surfaces with interaction between adsorbed molecules and it can be employed to describe the heterogeneous systems and may be written as follow:

$$q_e = K_F C_e^{1/n_F} \quad (7)$$

where K_F is the Freundlich constant indicative of the relative adsorption capacity of the adsorbent related to the bonding energy and can be defined as the adsorption or distribution coefficient. It represents the quantity of Cr^{6+} adsorbed onto adsorbent for unit equilibrium concentration. The constant n_F is the heterogeneity factor represents the deviation from linearity of adsorption as follows: if the value of $n_F = 1$, the adsorption is linear; $n_F < 1$, the adsorption process is chemical; if $n_F > 1$, the adsorption is a favorable physical process [31]. Eq. (7) can be linearized via logarithms in the form of Eq. (8) and the constants

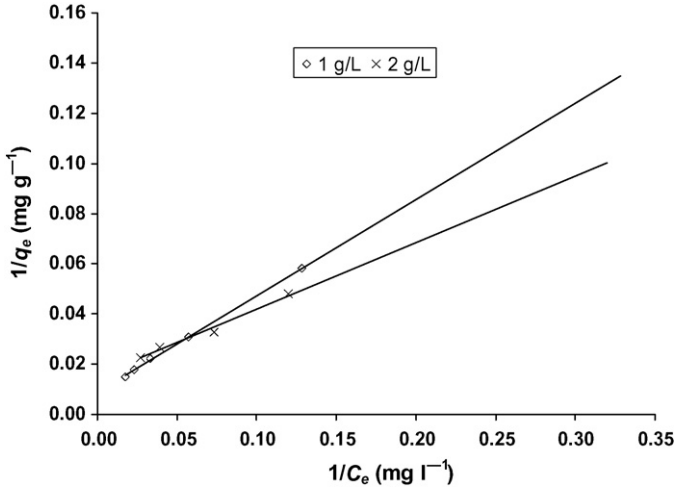

Fig. 5. Langmuir-2 isotherm model of Cr^{6+} adsorbed onto DSC.

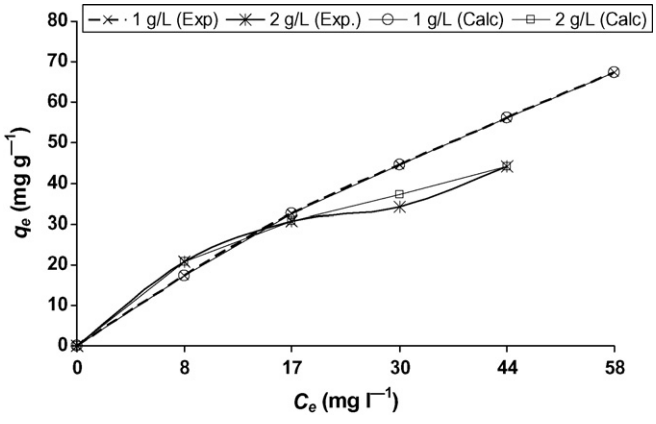

Fig. 6. Comparison between Langmuir equilibrium isotherms plots and the experimental data of Cr^{6+} adsorption on various dose of DSC.

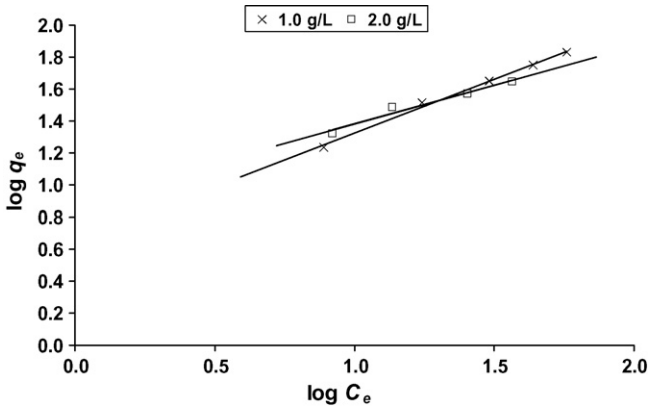

Fig. 7. Freundlich isotherm of Cr^{6+} adsorbed onto DSC.

can be determined.

$$\log q_e = \log K_F + \frac{1}{n_F}\log C_e \quad (8)$$

Fig. 7 represents the plot of $\log(q_e)$ versus $\log(C_e)$ with the intercept value of $\log K_F$ ($mg^{1-1/n}\,l^{1/n}\,g^{-1}$)and the slope of $1/n_F$ and are presented in Table 3. The correlation coefficients, $R^2 = 0.996$ and 0.962, obtained from Freundlich model is comparable to that obtained from Langmuir model linear forms 1 and 2, while it is slightly higher than that obtained from the linear forms 2 and 3. This result indicates that the experimental data fitted well to Freundlich model and the $n_F > 1$, indicating that adsorption of Cr^{6+} onto DSC is a favorable physical process [31].

Table 3
Comparison of the coefficients isotherm parameters for Cr^{6+} adsorption onto activated carbon developed from date palm seed

Isotherm model	Isotherm parameter	DSC dose	
		1.0 g l^{-1}	2.0 g l^{-1}
Freundlich	n_F	1.49	2.07
	K_F	4.48	7.85
	R^2	0.996	0.962
Koble–Corrigan	a	4.09	1.15
	b	0.01	0.02
	n	0.75	1.62
	R^2	0.998	1.000
Redlich–Peterson	A	17.9	5.03
	B	2.99	0.15
	g	0.385	0.847
	R^2	0.998	0.995
Tempkin	A_T	0.168	0.51
	B_T	28.82	14.92
	b_T	86.0	166.1
	R^2	0.980	0.983
Dubinin–Radushkevich	Q_m	64.62	43.03
	$K \times 10^6$	37.8	9.5
	E (kJ mol^{-1})	0.115	0.229
	R^2	0.898	0.963
Generalized isotherm	N_b	0.99	1.00
	K_G	46.53	16.13
	R^2	0.996	0.988

3.5.3. Koble–Corrigan isotherm

Koble–Corrigan equation is another isotherm model depends on the combination of the Langmuir and Freundlich equations in one non-linear equation for representing the equilibrium adsorption data. It is represented by Eq. (9) [35]:

$$q_e = \frac{aC_e^n}{1 + bC_e^n} \quad (9)$$

where a, b and n are the Koble–Corrigan parameters, which were obtained by solving Eq. (9) using SPSS version 10.0 computer program and reported in Table 3. The correlation coefficients obtained were 0.998 and 1.000 for adsorption of Cr^{6+} on DSC concentrations of 1.0 and 2.0 g l^{-1}, respectively. Fig. 8 shows the comparison between data calculated by Koble–Corrigan equation and the experimental data obtained for adsorption of different initial concentration of Cr^{6+} on DSC of doses 1.0 and 2.0 g l^{-1}. This indicates that Koble–Corrigan equation fit well to the experimental data obtained for adsorption of Cr^{6+} onto DSC. Also, the values of b were 0.01 and 0.02 indicate the combination between heterogeneous and homogeneous adsorption of Cr^{6+} on DSC.

3.5.4. Redlich–Peterson isotherm

A further empirical model has been developed by Redlich and Peterson [36] to improve the fit by Langmuir and Freundlich equations and this model equation is given by the non-linear Eq. (10).

$$q_e = \frac{AC_e}{1 + BC_e^g} \quad (10)$$

where A, B and g are the Redlich–Peterson parameters. The g value lies between zero and one. The constant g can characterize the isotherm as: if $g = 1$, the Langmuir will be the preferable isotherm, while if $g = 0$, the Freundlich will be the preferable isotherm. Although the two parameters in the Langmuir and Freundlich equations can be graphically determined, Redlich–Peterson constants is not applicable because of three unknown parameters so the three parameters in the equation are obtained using non-linear regression analysis included in SPSS program version 10.0 applicable to computer operation. The three isotherm constants A, B and g are reported

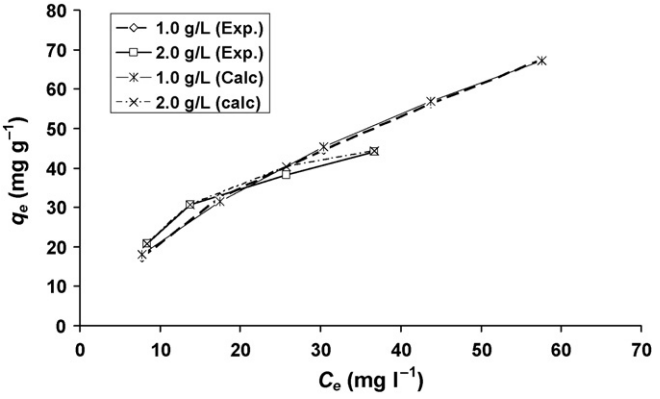

Fig. 8. Plot of q_e vs. C_e of experimental data and calculated q_e obtained from Koble–Corrigan isotherm model for the adsorption of Cr^{6+} onto DSC.

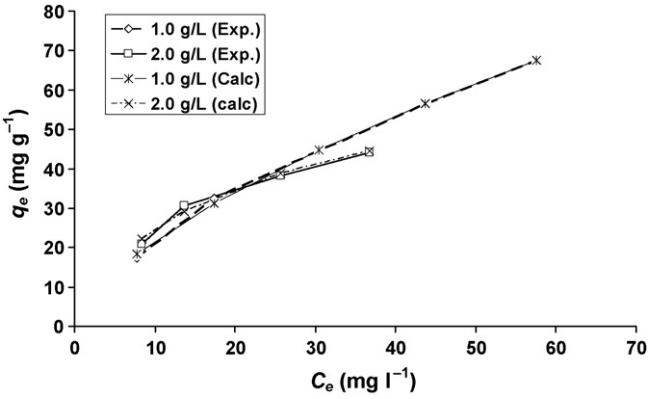

Fig. 9. Plot of q_e vs. C_e of experimental data and calculated q_e obtained Redlich–Peterson isotherm model for the adsorption of Cr^{6+} onto DSC.

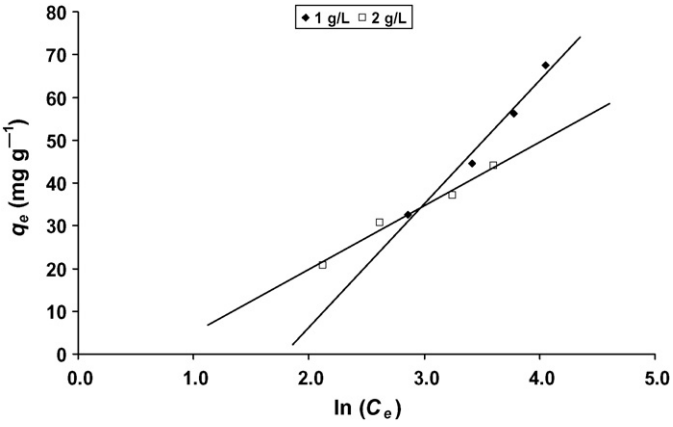

Fig. 10. Tempkin equilibrium isotherm model for the adsorption of Cr^{6+} onto DSC.

in Table 3. Fig. 9 shows the comparison between data calculated by Redlich–Peterson equation and the experimental data obtained for adsorption of different initial concentration of Cr^{6+} on 1.0 and 2.0 g l^{-1} doses of DSC. The correlation coefficients obtained (0.998 and 0.995) were comparable to the Langmuir and Freundlich equations indicating that the Redlich–Peterson isotherm can be consider as isotherm model for the data obtained from the adsorption of Cr^{6+} on DSC.

3.5.5. Tempkin isotherm

Tempkin isotherm equation [37] contains a factor that explicitly takes into account adsorbing species–adsorbate interactions. It assumes that: the heat of adsorption of all the molecules in the layer decreases linearly with coverage due to adsorbate–adsorbate repulsions and the adsorption is uniform distribution of maximum binding energy [38]. In addition, it assumes that the fall in the heat of sorption is linear rather than logarithmic, as implied in the Freundlich equation. It has commonly been written in the following Eq. (11) [39–41]:

$$q_e = \frac{RT}{b_T} \ln(A_T C_e) \quad \text{(non-linear form)} \tag{11}$$

$$q_e = B_T \ln A_T + B_T \ln C_e \quad \text{(linear form)} \tag{12}$$

where $B_T = (RT)/b_T$, T is the absolute temperature in *Kelvin* and R is the universal gas constant, 8.314 J mol^{-1} K^{-1}. The constant b_T is related to the heat of adsorption; A_T is the equilibrium binding constant (l min^{-1}) corresponding to the maximum binding energy [42,43]. The adsorption data can be analyzed according to Eq. (12). A plot of q_e versus ln C_e enables the determination of the isotherm constants A_T and b_T and represented in Fig. 10 and the value of constants and correlation coefficients are reported in Table 3. The correlation coefficients obtained are $R^2 \geq 0.98$, which indicates that the Tempkin isotherm fit well the equilibrium data obtained for the adsorption of Cr^{6+} onto DSC. However, based on the R^2 value, the Tempkin isotherm appears to be less applicable than Koble–Corrigan and Redlich–Peterson isotherm models.

3.5.6. Dubinin–Radushkevich (D–R) isotherm

Another equation used in the analysis of isotherms was proposed by Dubinin and Radushkevich [44]. It does not assume a homogeneous surface or constant sorption potential, but it applied to estimate the porosity apparent free energy and the characteristic of adsorption and it has commonly been applied in the following forms [45–47]:

$$q_e = Q_m \exp(-K\varepsilon^2) \quad \text{(non-linear form)} \tag{13}$$

$$\ln q_e = \ln Q_m - K\varepsilon^2 \quad \text{(linear form)} \tag{14}$$

where K is a constant related to the adsorption energy, Q_m the maximum adsorption capacity, ε can be calculated from Eq. (15).

$$\varepsilon = RT \ln\left(1 + \frac{1}{C_e}\right) \tag{15}$$

Fig. 11 shows D–R curves generated using Eq. (14) by plot of ln q_e versus ε^2 of the experimental data for the adsorption of Cr^{6+} by DSC. The constants K (mol^2 kJ^{-2}) and Q_m (mg g^{-1}) calculated from the slope and the intercept, respectively, and reported in Table 3. The mean free energy of adsorption (E) is the free energy change when one mole of ion transferred from infinity in solution to the surface of the sorbent. E is calculated

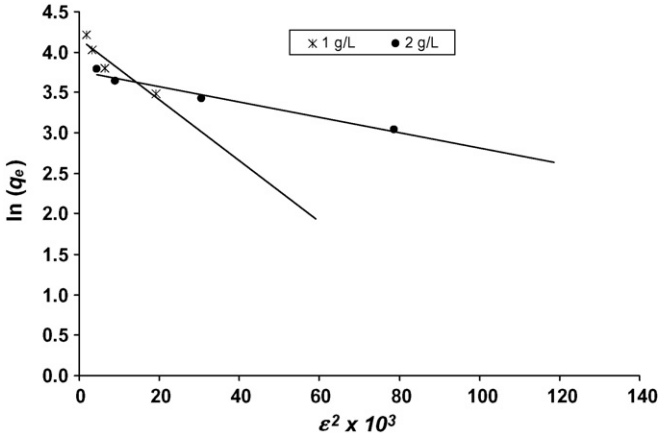

Fig. 11. Dubinin and Radushkevich isotherm model plots for the adsorption of Cr^{6+} by DSC.

from the K value using Eq. (16) [48]:

$$E = \frac{1}{\sqrt{(2K)}} \tag{16}$$

The values of correlation coefficients (0.898 and 0.963) indicate that the D–R is less fitting to the experimental data in comparable with the Langmuir, Freundlich, Koble–Corrigan and Tempkin isotherm models. The maximum capacity, Q_m, obtained using D–R isotherm model for adsorption of Cr^{6+} is 64.62 mg g^{-1} by DSC dose of 1.0 g l^{-1} (Table 3), which is about half of the Q_m obtained (120.48 mg g^{-1}) by Langmuir-1 isotherm model (Table 2). The values of E calculated using Eq. (16) are 0.115 and 0.229 kJ mol^{-1}, while the typical E values for ion-exchange mechanisms are ranged between 8 and16 kJ mol^{-1}, indicating that the adsorption process of Cr^{6+} ion onto DSC is physisorption, which is in agreement with the result obtained from the pH study.

3.5.7. Generalized isotherm equation

A generalized isotherm equation was tested for correlation of the equilibrium data [49–51]. Linear form of the generalized isotherm is given by:

$$\log\left[\frac{Q_m}{q_e} - 1\right] = \log K_G - N_b \log C_e \tag{17}$$

where K_G is the saturation constant (mg l^{-1}); N_b the cooperative binding constant; Q_m the maximum adsorption capacity of the adsorbent (mg g^{-1}) (obtained from Langmuir isotherm model); q_e (mg g^{-1}) and C_e (mg l^{-1}) are the equilibrium chromium concentrations in the solid and liquid phases, respectively. Fig. 12 shows a plot of $\log[(Q_m/q_e) - 1]$ versus $\log C_e$; the intercept gave $\log K_G$ and the slope gave N_b constants. Parameters related to each isotherm were determined by using linear regression analysis and the square of the correlation coefficients (R^2) have been calculated. A list of the parameters obtained together with R^2 values is given in Table 3. Apparently, the generalized adsorption isotherm represents the equilibrium data reasonably well. The exponent (K_G) was 0.99 and 1.0 which reflects that the generalized isotherm approximates to the Langmuir expression.

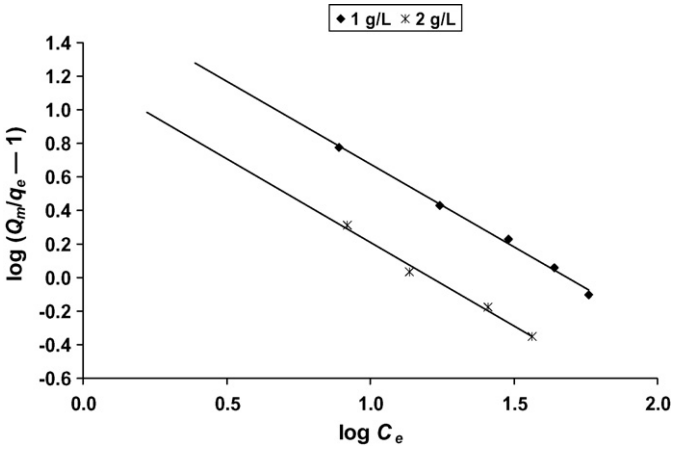

Fig. 12. Generalized isotherm model.

The data reported in Tables 2 and 3 showed that most of the isotherm models tested have been fitted well the experimental data obtained for the adsorption of Cr^{6+} on DSC. Only, Dubinin–Radushkevich isotherm showed less agreement with the experimental data obtained.

3.6. Adsorption kinetic considerations

Batch experiments were conducted to explore the rate of Cr^{6+} adsorption by DSC at pH 1.0, DSC of 1, 2, 3, 4, 5 g l^{-1} and initial metal concentrations of 25, 50, 75, 100 and 125 mg l^{-1}. The kinetic adsorption data can be processed to understand the dynamics of the adsorption reaction in terms of the order of the rate constant. The process of metal removal from aqueous phase by a certain adsorbent may be investigated by several models to examine the rate-controlling of the adsorption process such as chemical reaction, diffusion control and mass transfer. Since the kinetic parameters are used to predict the adsorption rate and give important information for designing and modeling of the adsorption processes, the kinetics of the adsorption of chromium onto DSC was investigated for selecting optimum operating conditions for a full-scale batch process. Pseudo first-order [52], pseudo second-order [53], Elovich [54–56] and intraparticle diffusion [57,58] kinetic models were applied for the adsorption of Cr^{6+} on DSC and the conformity between experimental data and the model-predicted values was expressed by the correlation coefficients (R^2).

3.6.1. Pseudo first-order equation

The Lagergren pseudo-first-order model [52] is the earliest known equation describing the adsorption rate based on the adsorption capacity. The differential equation is commonly expresses as follows:

$$\frac{dq_t}{dt} = k_1(q_e - q_t) \tag{18}$$

where q_e and q_t refer to the amount of Cr^{6+} adsorbed (mg g^{-1}) at equilibrium and at any time, t (min), respectively, and k_1 is the equilibrium rate constant of pseudo first-order adsorption (l min^{-1}). Integrating Eq. (18) for the boundary conditions $t = 0$ to t and $q_t = 0$ to q_t gives:

$$\log\left(\frac{q_e}{q_e - q_t}\right) = \frac{k_1}{2.303}t \tag{19}$$

which is the integrated rate law for a pseudo first-order reaction. Eq. (19) can be rearranged to obtain the linear form:

$$\log(q_e - q_t) = \log(q_e) - \frac{k_1}{2.303}t \tag{20}$$

Values of the rate constant, k_1, equilibrium adsorption capacity, q_e, and the correlation coefficient, R^2, were calculated from the plots of $\log(q_e - q_t)$ versus t (Fig. 13). Although the correlation coefficients obtained from pseudo first-order model are found to be high the calculated q_e do not agree with experimental values (Table 4). This indicates that adsorption of Cr^{6+} onto DSC is not an ideal pseudo-first-order reaction [31].

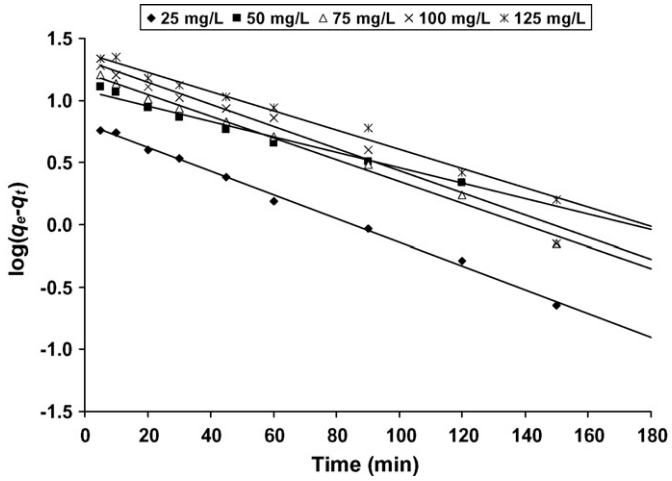

Fig. 13. Pseudo first-order kinetics for Cr^{6+} adsorption onto DSC. Conditions: adsorbent dosage 3 g l^{-1}, pH 1.0, temperature 27 ± 2 °C.

3.6.2. Pseudo second-order equation

Kinetic data were further treated with the pseudo-second-order kinetic model [53]. The differential equation is commonly given as following:

$$\frac{dq_t}{dt} = k_2(q_e - q_t)^2 \quad (21)$$

where k_2 (g mg^{-1} min^{-1}) is the equilibrium rate constant of pseudo-second-order adsorption. Integrating Eq. (21) for the boundary conditions $q_t = 0$ to q_t and $t = 0$ to t gives:

$$\left(\frac{t}{q_t}\right) = \frac{1}{k_2 q_e^2} + \frac{1}{q_e}(t) \quad (22)$$

The initial adsorption rate, h (mg g^{-1} min^{-1}) is expressed by the following Eq. (23):

$$h = k_2 q_e^2 \quad (23)$$

If pseudo-second-order kinetics is applicable, the plot of t/q_t versus t should show a linear relationship. The linear plot t/q_t versus t shows a good agreement of the experimental data with the pseudo-second-order kinetic model for adsorption of Cr^{6+} on DSC (Fig. 14). The correlation coefficients (R^2) for the second-order kinetics model are higher than 0.99. The second order rate constant, k_2, and the equilibrium adsorption capacity, q_e, were calculated from the intercept and slope of the plots of t/q_t versus t. The calculated q_e values agree very well with the experimental data (Table 4). These indicate that the adsorption of Cr^{6+} from aqueous solution on DSC obeys pseudo-second-order kinetic model.

The values of initial adsorption rate (h) that represents the rate of initial adsorption, is practically increased with the increase in initial chromium concentrations, while the pseudo-second-order rate constant (k_2) decreased with increasing of initial chromium concentration from 25 to 125 mg l^{-1} (Table 4).

Table 4
Comparison of the first- and second-order adsorption rate constants and calculated and experimental q_e values for different initial Cr^{6+} and activated carbon developed from date palm seed

Parameter			First-order kinetic model			Second-order kinetic model			
DSC dose (g l^{-1})	Cr^{6+} (mg l^{-1})	q_e (exp.)	$k_1 \times 10^3$	q_e (calc.)	R^2	$k_2 \times 10^3$	q_e (calc.)	h	R^2
	25	17.22	18.19	17.26	0.971	2.87	18.38	0.97	0.999
	50	32.56	13.59	22.61	0.976	1.41	33.00	1.53	0.994
1.0	75	44.61	11.98	25.06	0.945	1.58	43.67	3.01	0.994
	100	56.28	10.59	33.85	0.978	1.09	54.05	3.19	0.990
	125	67.45	12.90	38.04	0.979	1.01	67.11	4.55	0.993
	25	12.50	13.82	9.50	0.990	2.53	13.37	0.45	1.000
	50	20.83	19.11	17.22	0.988	1.50	23.58	0.83	0.993
2.0	75	30.65	12.90	21.30	0.986	1.55	30.86	1.48	0.993
	100	37.26	16.12	25.32	0.991	1.23	36.63	1.52	0.991
	125	44.13	13.82	27.61	0.926	1.13	41.84	2.33	0.997
	25	8.33	21.88	6.46	0.996	4.32	9.43	0.38	0.999
	50	16.67	14.28	12.07	0.984	2.30	17.54	0.71	0.998
3.0	75	23.44	20.04	16.78	0.992	2.06	25.45	1.33	0.996
	100	27.46	20.50	21.26	0.973	1.57	30.00	1.41	0.993
	125	34.65	17.73	24.26	0.988	1.36	37.04	1.86	0.993
	25	6.25	21.88	4.84	0.996	5.78	7.07	0.29	0.999
	50	12.50	15.89	11.88	0.989	4.36	13.48	0.79	0.999
4.0	75	18.75	19.81	8.11	0.989	2.88	19.69	1.11	0.997
	100	23.13	16.58	15.13	0.990	2.14	24.69	1.30	0.995
	125	27.25	19.81	18.54	0.988	1.97	29.24	1.69	0.995
	25	5.00	37.77	3.09	0.978	23.1	5.27	0.64	1.000
	50	10.00	25.56	6.47	0.988	6.94	10.81	0.81	0.999
5.0	75	15.00	19.11	8.91	0.981	4.24	15.95	1.08	0.999
	100	18.90	26.48	12.40	0.979	4.12	20.08	1.66	0.999
	125	23.11	18.42	13.30	0.992	2.97	24.33	1.76	0.998

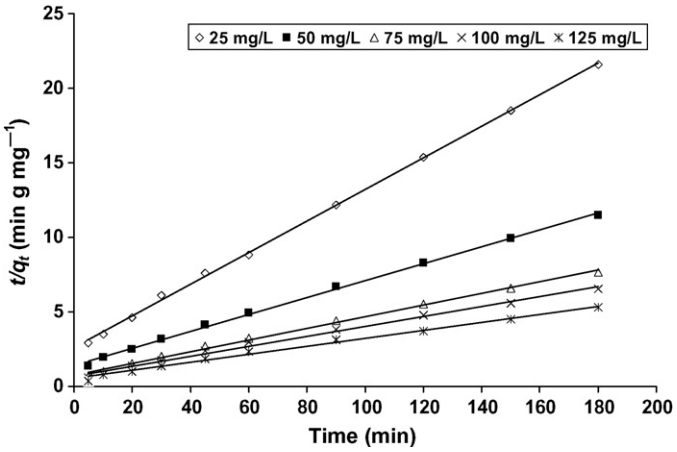

Fig. 14. Plot of the pseudo-second-order model at different initial Cr^{6+} concentrations, CDS 3.0 g l^{-1}, pH 1.0, temperature 27 ± 2 °C.

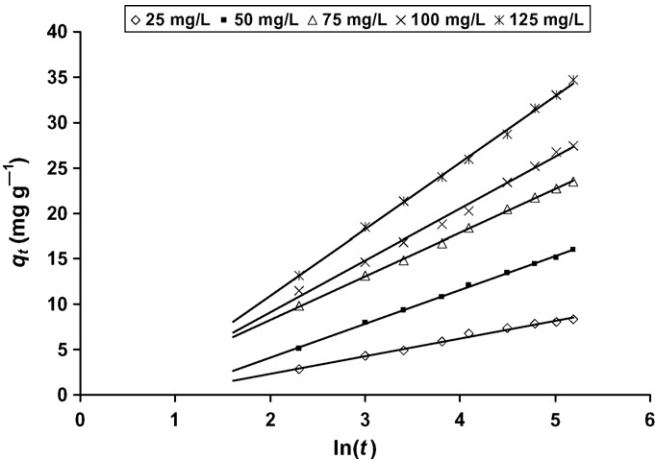

Fig. 15. Elovich model plot for the adsorption of Cr^{6+} onto DSC (6.0 g l^{-1}) at different initial Cr^{6+} concentrations (25, 50, 75, 100 and 125 mg l^{-1}).

3.6.3. Elovich kinetic equation

Elovich equation is a rate equation based on the adsorption capacity commonly expressed as following Eq. (24) [54–56]:

$$\frac{dq_t}{dt} = \alpha \exp(-\beta q_t) \quad (24)$$

where α is the initial adsorption rate (mg g^{-1} min^{-1}) and β the desorption constant (g mg^{-1}) related to the extent of surface coverage and activation energy for chemisorption. Eq. (24) is simplified by assuming $\alpha\beta \gg t$ and by applying the boundary conditions $q_t = 0$ at $t = 0$ and $q_t = q_t$ at $t = t$ becomes:

$$q_t = \frac{1}{\beta}\ln(\alpha\beta) + \frac{1}{\beta}\ln(t) \quad (25)$$

Fig. 15 depicts plot of q_t versus $\ln(t)$ and the Elovich constants α and β were obtained from the intercept and slope, respectively, and reported in Table 5. The correlation coefficients R^2 are higher than 0.99, which is comparable to correlation coefficients obtained for pseudo-second-order model. This reflects the applicability of this model to the

Table 5
The parameters obtained from Elovich kinetics model and intraparticle diffusion model using different initial Cr^{6+} concentrations and DSC doses

DSC dose (g l^{-1})	Cr^{6+} concentration	Elovich			Intraparticle diffusion		
		β	α	R^2	K_{dif}	C	R^2
1.0	25	0.19	8.58	0.993	1.29	0.39	0.976
	50	0.13	4.64	0.992	2.02	6.08	0.975
	75	0.11	5.39	0.992	2.40	12.17	0.979
	100	0.10	5.12	0.994	2.70	17.05	0.985
	125	0.09	4.37	0.998	3.07	25.65	0.992
2.0	25	0.35	1.00	0.994	0.80	1.96	0.982
	50	0.20	1.83	0.993	1.42	3.11	0.967
	75	0.16	3.38	0.994	1.82	6.18	0.984
	100	0.14	4.03	0.992	1.99	8.10	0.996
	125	0.11	4.78	0.995	2.55	12.53	0.999
3.0	25	0.51	0.88	0.991	0.53	2.07	0.979
	50	0.26	1.60	0.996	0.97	3.81	0.978
	75	0.21	3.68	0.999	1.28	7.62	0.985
	100	0.18	3.78	0.992	1.50	8.37	0.988
	125	0.14	4.39	0.998	1.82	11.03	0.993
4.0	25	0.67	0.62	0.994	0.45	1.06	0.970
	50	0.38	1.95	0.997	0.83	3.30	0.973
	75	0.27	3.02	0.998	1.12	5.16	0.981
	100	0.21	3.55	0.998	1.23	7.37	0.979
	125	0.19	5.06	1.000	1.64	7.74	0.983
5.0	25	1.16	2.92	0.990	0.24	2.34	0.783
	50	0.31	7.19	0.997	0.56	3.57	0.890
	75	0.35	3.41	0.992	0.84	4.89	0.900
	100	0.49	2.32	0.996	0.95	7.60	0.915
	125	0.25	7.24	0.998	1.02	10.21	0.963

experimental data obtained for the adsorption of Cr^{6+} on DSC.

3.6.4. Intraparticle diffusion model

Adsorption of any metal ions from aqueous phase onto solid phase is a multi-step process involving transport of metal ions from aqueous phase to the surface of the solid particles (bulk diffusion) and then, diffusion of metal ions via the boundary layer to the surface of the solid particles (film diffusion) followed by transport of metal ions from the solid particles surface to its interior pores (pore diffusion or intraparticle diffusion), which is likely to be a slow process, therefore, it may be the rate-determining step. In addition, adsorption of metal ion at an active site on the solid phase surface could also be occurred and called chemical reaction such as ion-exchange, complexation and chelation. The metal ion adsorption is controlled usually by either the intraparticle (pore diffusion) or the liquid-phase mass transport rates [31]. If the experiment is a batch system with rapid stirring, there is a possibility that intraparticle diffusion is the rate-determining step [59]. Weber and Morris [57] provided the rate for intraparticle diffusion by relationship between q_t and the square root of time, $t^{1/2}$, as depicted in Eq. (26).

$$q_t = K_{dif} t^{1/2} + C \quad (26)$$

where K_{dif} (mg g^{-1} min^{-1}) is the intraparticle diffusion rate constant and C (mg g^{-1}) is related to the thickness of the boundary layer, and K_{dif} and C values are calculated from the slope and intercept of q_t versus $t^{1/2}$ plots, respectively.

Since the chromium is probably transported from its aqueous solution to the DSC by intraparticle diffusion, so the intraparticle diffusion is another kinetic model should be used to study the rate-determining step for Cr^{6+} adsorption onto DSC. Plot of q_t versus $t^{1/2}$ for adsorption of Cr^{6+} (25–125 mg l^{-1}) on DSC (1.0 g l^{-1}) were depicted in Fig. 16, and the values of K_{dif} and C are reported in Table 5.

If the intraparticle diffusion is involved in the adsorption process, then the plot of q_t versus $t^{1/2}$ would result in a linear relationship, and the intraparticle diffusion would be the

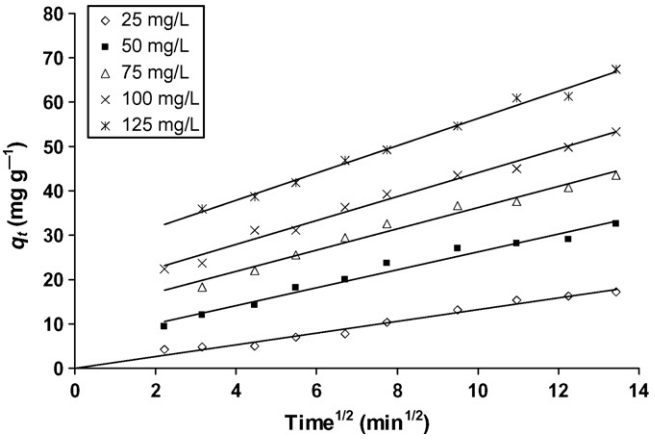

Fig. 16. Intraparticle diffusion model plot for the adsorption of Cr^{6+} onto DSC (1.0 g l^{-1}) at different initial Cr^{6+} concentration (25, 50, 75, 100 and 125 mg l^{-1}) and room temperature.

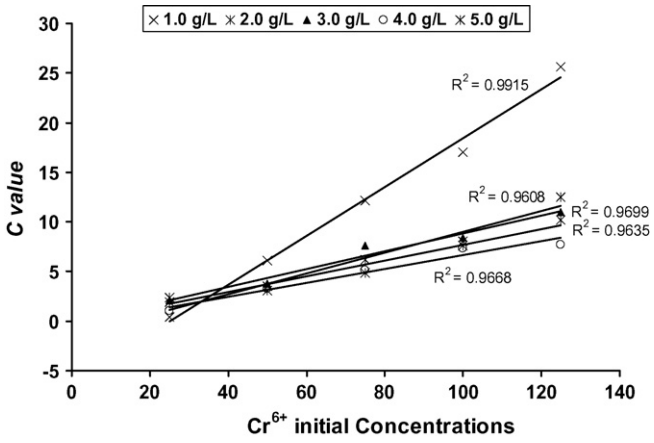

Fig. 17. Plot of Cr^{6+} initial concentrations (25, 50, 75, 100 and 125 mg l^{-1}) vs. thickness of boundary layer C value obtained for different DSC doses at room temperature.

controlling step if this line passed through the origin [31]. The shape of Fig. 16 confirms strait lines not passed through the origin for most studied initial concentrations of Cr^{6+} except for 25 mg l^{-1}. The correlation coefficients are higher than 0.97 for all studied DSC doses except for 5 g l^{-1}. These results indicate that the intraparticle diffusion is the only rate determine step for the 25 mg l^{-1} initial Cr^{6+} concentration, while there are some degree of boundary layer for the higher initial concentration, which indicate that the intraparticle diffusion is not only the rate controlling step for the adsorption of the Cr^{6+} on DSC for higher initial concentrations (50–125 mg l^{-1}).

On the other hand, Fig. 17 depicts the plot between C versus initial Cr^{6+} concentrations for different DSC doses. The C value was found to increase with increase of initial Cr^{6+} concentration, which indicated increase of the thickness of the boundary layer and decrease of the chance of the external mass transfer and hence increase of the chance of internal mass transfer. The C values were found to decrease with increase of DSC dose, which reflect decrease of the thickness of the boundary layer and hence increase of the chance of the external mass transfer. The intraparticle diffusion rate constant, K_{dif}, were in the range of 0.24–3.7 mg g^{-1} min^{-1} and it increase with increase of initial chromium concentration and decrease of DSC dose.

3.7. Applicability on real wastewater and saline water

The applicability of chromium removal on DSC was tested using artificial and natural seawater and real wastewater. Table 6 shows that the percentage of chromium removal by DSC from aqueous solution was not affected by replacing the distilled water by artificial seawater, natural seawater or wastewater. A near 90% removal of toxic chromium from synthetic seawater, natural seawater and wastewater was detected for activated carbon developed from date palm seed. Moreover, the maximum adsorption capacities were not significantly changed by changing of the type of chromium solution. The presence of salt had no effect on the removal of chromium by DSC, which leads to deduce that there was no interaction between the salt and the

Table 6
Data obtained for the adsorption of chromium (125 mg l^{-1}) from different solution using DSC (5.0 g l^{-1})

Solution of chromium used	DSC	
	Removal (%)	Maximum capacity (mg g^{-1})
Distilled water	92.43	120.48
Artificial seawater	93.12	121.22
Natural seawater	91.25	118.78
Wastewater	90.84	118.49

DSC nor the salt and the Cr^{6+}. Also, the high concentration of chromium ions may make them more preferable to adsorb by DSC. On the other hand, the real wastewater may contain very low concentrations from several pollutants that will not have much effect on the removal efficiency of chromium ions. These results indicates that the new developed carbon from date palm seed are applicable material for removal of Cr^{6+} ions from different types of aqueous solutions including wastewater.

4. Conclusion

The present study indicates that new carbon developed from date palm seed (DSC) is an effective adsorbent for the removal of toxic chromium from different kinds of aqueous solution. The physico-chemical characteristics of DSC surface having an excess of positive charge enabled activated carbon to adsorb toxic chromium with a great capacity. With respect to the suitability of the first-order and second-order kinetic models for chromium adsorption on DSC, it has been found that the adsorption kinetics of chromium preferably obeys the second-order kinetic models, which provides the higher correlation coefficient and calculated q_e agree well with the experimental data. However, the adsorption of chromium on DSC is a complex process and cannot be adequately described by a single kinetic model throughout the whole process. Therefore, the Elovich model and intraparticle diffusion were investigated. The intraparticle diffusion played a significant role, but it was not the main rate-determining step during adsorption of chromium on DSC except for the 25 mg l^{-1} initial chromium concentration, where the intraparticle diffusion was the rate-determining step. By comparing the correlation coefficients obtained for studied isotherm models, all isotherm models were fit the experimental data reasonably well except Dubinin–Radushkevich isotherm model. The DSC exhibited maximum adsorption capacity of 120.42 mg l^{-1}, which is comparable with that reported in literature. The percentage removal and maximum adsorption capacity were not affected by sodium chloride ions in the solution or by replacing the distilled water by natural seawater or real wastewater. Since the raw material date palm seed is freely available in large quantities as a waste in jam industries, the treatment method seems to be economical. Based on the above good results this relatively cheap, low-cost DSC is recommended as an effective and cheap adsorbent for removal of chromium from industrials effluents.

References

[1] G. Rich, K. Cherry, Hazardous Waste Treatment Technology, Pudvan Publishing Co., Northbrook, IL, 1987, p. 182.
[2] B. Volesky, Biosorption of Heavy Metals, CRC Press, Boston, USA, 1990, p. 408, ISBN 0849349176.
[3] M.C. Basso, E.G. Cerrella, A.L. Cukierman, Empleo de algas marinas para la biosorción de metales pesados de aguas contaminadas, Avances en Energías Renovables Medio Ambiente 6 (2002), ISSN 0329-5184.
[4] Z. Aksu, F. Gönen, Z. Demircan, Biosorption of chromium(VI) ions by Mowital B3OH resin immobilized activated sludge in a packed bed: comparison with granular activated carbon, Process. Biochem. 38 (2002) 175–186.
[5] S. Babel, T.A. Kurniawan, Low-cost adsorbents for heavy metals uptake from contaminated water: a review, J. Hazard. Mater. B97 (2003) 219–243.
[6] A. Baran, E. Biçak, S.H. Baysal, S. Önal, Comparative studies on the adsorption of Cr(VI) ions on to various sorbents, Bioresour. Technol. 98 (2006) 661–665.
[7] A. El-Sikaily, A. El Nemr, A. Khaled, O. Abdelwahab, Removal of toxic Chromium from wastewater using green alga *Ulva lactuca* and its activated Carbon, J. Hazard. Mater., in press.
[8] O. Abdelwahab, A. El Nemr, A. El-Sikaily, A. Khaled, Biosorption of Direct Yellow 12 from aqueous solution by marine green algae *Ulva Lactuca*, Chem. Ecol. 22 (2006) 253–266.
[9] A. El-Sikaily, A. Khaled, A. El Nemr, O. Abdelwahab, Removal of methylene blue from aqueous solution by marine green alga *Ulva lactuca*, Chem. Ecol. 22 (2006) 149–157.
[10] A. El Nemr, A. El-Sikaily, A. Khaled, O. Abdelwahab, Removal of toxic chromium(VI) from aqueous solution by activated carbon developed from *Casuarina Equisetifolia*, Chem. Ecol. 23 (2) (2007) 119–129.
[11] O. Abdelwahab, A. El-Sikaily, A. Khaled, A. El Nemr, Mass transfer processes of chromium(VI) adsorption onto Guava seeds, Chem. Ecol. 23 (1) (2007) 73–85.
[12] S. Mor, K. Ravindra, N.R. Bishnoi, Adsorption of chromium from aqueous solution by activated alumina and activated charcoal, Bioresour. Technol. 98 (2007) 954–957.
[13] C.Y. Yin, M.K. Aroua, W.M.A.W. Daud, Review of modifications of activated carbon for enhancing contaminant uptakes from aqueous solutions, Sep. Purif. Technol. 52 (2007) 403–415.
[14] F. Gode, E. Pehlivan, Removal of Cr(VI) from aqueous solution by two Lewatit-anion exchange resins, J. Hazard. Mater. B119 (2005) 175–182.
[15] C. Pellerin, S.M. Booker, Reflection on hexavalent chromium, health hazards of an industrial heavyweight, Environ. Health Perspect. 108 (9) (2000) 402–407.
[16] Y.G. Ko, U.S. Choi, T.Y. Kim, D.J. Ahn, Y.J. Chn, FT-IR and isotherm study on anion adsorption onto novel chelating fibers, Macromol. Rapid Commun. 23 (2002) 535–539.
[17] R. Codd, C.T. Dillon, A. Levina, P.A. Lay, Studies on the genotoxicity of chromium: from the test tube to the cell, Coord. Chem. Rev. 216–217 (2001) 537–582.
[18] R.L. Ramos, A.J. Martinez, R.M.G. Coronado, Adsorption of chromium(VI) from aqueous solutions on activated carbon, Water Sci. Technol. 30 (9) (1994) 191–197.
[19] F.C. Richad, A.C.M. Bourg, Aqueous geochemistry of chromium: a review, Water Res. 25 (7) (1991) 807–816.
[20] EPA, USEPA Report no. EPA/570/9-76/003; Washington, DC, 1976.
[21] R.R. Patterson, S. Fendorf, M. Fendorf, Reduction of hexavalent chromium by amorpous iron sulfide, Environ. Sci. Technol. 31 (1997) 2039–2044.
[22] F.W. Gilcreas, M.J. Tarars, R.S. Ingols, Standard Methods for the Examination of water and wastewater, 12th ed., American Public Health Association (APHA) Inc., New York, 1965, p. 213.
[23] C. Raji, T.S. Anirudhan, Batch Cr(VI) removal by polyacrylamide-grafted sawdust: kinetics and thermodynamics, Water Res. 32 (12) (1998) 3772–3780.
[24] B.M. Weckhuysen, I.E. Wachs, R.A. Schoonheydt, Surface chemistry and spectroscopy of chromium in inorganic oxides, Chem. Rev. 96 (1996) 3327–3349.

[25] S. Mor, K. Ravindra, N.R. Bishnoi, Adsorption of chromium from aqueous solution by activated alumina and activated charcoal, Biroresour. Technol. 98 (2007) 954–957.
[26] K. Selvi, S. Pattabhi, K. Kadirvelu, Removal of Cr(VI) from aqueous solution by adsorption onto activated carbon, Bioresour. Technol. 80 (2001) 87–89.
[27] J.M. Smith, Chemical Engineering Kinetics, third ed., McGraw-Hill, Singapore, 1981.
[28] I. Langmuir, The constitution and fundamental properties of solids and liquids, J. Am. Chem. Soc. 38 (1916) 2221–2295.
[29] I. Langmuir, The adsorption of gases on plane surfaces of glass, mica and platinum, J. Am. Chem. Soc. 40 (1918) 1361–1403.
[30] M. Doğan, M. Alkan, Y. Onganer, Adsorption of methylene blue from aqueous solution onto perlite, Water Air Soil Pollut. 120 (2000) 229–249.
[31] G. Crini, H.N. Peindy, F. Gimbert, C. Robert, Removal of C.I. Basic Green 4 (Malachite Green) from aqueous solutions by adsorption using cyclodextrin-based adsorbent: kinetic and equilibrium studies, Sep. Purif. Technol. 53 (2007) 97–110.
[32] D.G. Kinniburgh, General purpose adsorption isotherms, Environ. Sci. Technol. 20 (1986) 895–904.
[33] E. Longhinotti, F. Pozza, L. Furlan, M.D.N.D. Sanchez, M. Klug, M.C.M. Laranjeira, V.T. Favere, Adsorption of anionic dyes on the biopolymer chitin, J. Brazil. Chem. Soc. 9 (1998) 435–440.
[34] H.M.F. Freundlic, Über die adsorption in lösungen, Zeitschrift für Physikalische Chemie (Leipzig) 57A (1906) 385–470.
[35] R.A. Koble, T.E. Corrigan, Adsorption isotherm for pure hydrocarbons, Ind. Eng. Chem. 44 (1952) 383–387.
[36] O. Redlich, D.L. Peterson, A useful adsorption isotherm, J. Phys. Chem. 63 (1959) 1024–1026.
[37] M.J. Tempkin, V. Pyzhev, Acta Physiochim. URSS 12 (1940) 217–222.
[38] D. Kavitha, C. Namasivayam, Experimental and kinetic studies on methylene blue adsorption by coir pith carbon, Bioresour. Technol. 98 (2007) 14–21.
[39] C. Aharoni, D.L. Sparks, Kinetics of soil chemical reactions—a theoretical treatment, in: D.L. Sparks, D.L. Suarez (Eds.), Rate of Soil Chemical Processes, Soil Science Society of America, Madison, WI, 1991, pp. 1–18.
[40] C. Aharoni, M. Ungarish, Kinetics of activated chemisorption. Part 2. Theoretical models, J. Chem. Soc., Faraday Trans. 73 (1977) 456–464.
[41] X.S. Wang, Y. Qin, Equilibrium sorption isotherms for of Cu^{2+} on rice bran, Proc. Biochem. 40 (2005) 677–680.
[42] C.I. Pearce, J.R. Lioyd, J.T. Guthrie, The removal of color from textile wastewater using whole bacterial cells: a review, Dyes Pigments 58 (2003) 179–196.
[43] G. Akkaya, A. Ozer, Adsorption of acid red 274 (AR 274) on Dicranella varia: determination of equilibrium and kinetic model parameters, Proc. Biochem. 40 (11) (2005) 3559–3568.
[44] M.M. Dubinin, L.V. Radushkevich, Equation of the characteristic curve of activated charcoal, Chem. Zentr. 1 (1947) 875.
[45] L.V. Radushkevich, Potential theory of sorption and structure of carbons, Zhurnal Fizicheskoi Khimii 23 (1949) 1410–1420.
[46] M.M. Dubinin, The potential theory of adsorption of gases and vapors for adsorbents with energetically non-uniform surface, Chem. Rev. 60 (1960) 235–266.
[47] M.M. Dubinin, Modern state of the theory of volume filling of micropore adsorbents during adsorption of gases and steams on carbon adsorbents, Zhurnal Fizicheskoi Khimii 39 (1965) 1305–1317.
[48] S. Kundu, A.K. Gupta, Investigation on the adsorption efficiency of iron oxide coated cement (IOCC) towards As(V)—kinetics, equilibrium and thermodynamic studies, Colloids Surf. A: Physicochem. Eng. Aspects 273 (2006) 121–128.
[49] F. Kargi, S. Ozmichi, Biosorption performance of powdered activated sludge for removal of different dyestuffs, Enzyme Microb. Technol. 35 (2004) 267–271.
[50] S. Ozmihci, F. Kargi, Utilization of powdered waste sludge (PWS) for removal of textile dyestuffs from wastewater by adsorption, J. Environ. Manage. 81 (2006) 307–314.
[51] F. Kargi, S. Cikla, Biosorption of zinc(II) ions onto powdered waste sludge (PWS): kinetics and isotherms, Enzyme Microb. Technol. 38 (2006) 705–710.
[52] S. Lagergren, Zur theorie der sogenannten adsorption geloster stoffe, Kungliga Svenska Vetenskapsakademiens, Handlingar 24 (1898) 1–39.
[53] Y.S. Ho, G. McKay, D.A.J. Wase, C.F. Foster, Study of the sorption of divalent metal ions on to peat, Adsorp. Sci. Technol. 18 (2000) 639–650.
[54] J. Zeldowitsch, Über den mechanismus der katalytischen oxidation von CO and MnO_2, Acta Physicochim. URSS 1 (1934) 364–449.
[55] S.H. Chien, W.R. Clayton, Application of Elovich equation to the kinetics of phosphate release and sorption on soils, Soil. Sci. Soc. Am. J. 44 (1980) 265–268.
[56] D.L. Sparks, Kinetics of Reaction in Pure and Mixed Systems, in Soil Physical Chemistry, CRC Press, Boca Raton, 1986.
[57] W.J. Weber, J.C. Morris, Kinetics of adsorption on carbon from solution, J. Sanity Eng. Div. Am. Soc. Civil Eng. 89 (1963) 31–59.
[58] K. Srinivasan, N. Balasubramanian, T.V. Ramakrishan, Studies on chromium removal by rice husk carbon, Indian J. Environ. Health 30 (1988) 376–387.
[59] G. McKay, The adsorption of dyestuff from aqueous solution using activated carbon: analytical solution for batch adsorption based on external mass transfer and pore diffusion, Chem. Eng. J. 27 (1983) 187–195.